Iranian Journal of Basic Medical Sciences
ijbms.mums.ac.ir

Quercetin attenuates ferroptosis-associated myocardial injury in rats after coronary microembolization by activating the Nrf2/HO-1 signaling pathway

Junwen Huang [1], Zhiqi Tang [1], Jiacong Nong [1], Guangpeng Tu [1], Xueyi Feng [1], Lang Li [1]*

[1] Department of Cardiology, The First Affiliated Hospital of Guangxi Medical University, Guangxi Cardiovascular Institute, Nanning 530021, Guangxi, China

ARTICLE INFO

Article type:
Original

Article history:
Received: Aug 25, 2025
Accepted: Jun 17, 2026

Keywords:
Coronary-microembolization
Ferroptosis
Nrf2/HO-1
Oxidative stress
Quercetin

ABSTRACT

Objective(s): Coronary microembolization (CME) significantly contributes to the progression of heart failure and is strongly associated with adverse clinical outcomes in patients. Ferroptosis has been implicated in CME-induced myocardial injury. Quercetin has well-documented anti-inflammatory and antioxidant properties and shows therapeutic potential in coronary artery disease. However, its precise mechanism for regulating ferroptosis during CME-mediated myocardial injury remains unclear. This study aims to elucidate the therapeutic effects of quercetin and its underlying molecular mechanisms that regulate ferroptosis in cardiomyocytes following CME.

Materials and Methods: The Sprague-Dawley(SD) rats were randomly divided into four groups (n=7 each): Sham, CME, CME+Quercetin (Que), and CME+Quercetin+ML385 (Que+ML385). The CME model was produced by injecting microspheres into the left ventricles. We administered pharmacological treatments as follows: The Que and Que+ML385 groups received daily oral quercetin (250 mg/kg) starting 7 days before model induction until the procedure day. Additionally, we pretreated the Que+ML385 group with intraperitoneal injection of ML385 (30 mg/kg) 2 hr before CME induction. The comprehensive evaluations include cardiac function assessment, quantification of serum biomarkers of myocardial injury, cardiac tissue histology, and analysis of ferroptosis-related molecular markers to evaluate quercetin's therapeutic effects.

Results: Quercetin pretreatment significantly improved cardiac function, reduced serum markers of myocardial injury, and decreased microinfarction size. At the molecular level, quercetin up-regulated Nrf2 and HO-1 expression and attenuated biochemical markers of cardiomyocyte ferroptosis. However, ML385 co-treatment attenuated this protective effect.

Conclusion: Quercetin may inhibit ferroptosis in cardiomyocytes by activating the Nrf2/HO-1 signaling pathway, thereby improving CME-related cardiac dysfunction and reducing myocardial injury.

▶ Please cite this article as:
Huang J, Tang Zh, Nong J, Tu G, Feng X, Li L. Quercetin attenuates ferroptosis-associated myocardial injury in rats after coronary microembolization by activating the Nrf2/HO-1 signaling pathway. Iran J Basic Med Sci 2026; 29: 1361-1368. doi: https://dx.doi.org/10.22038/ijbms.2026.90613.19556

Introduction

Coronary microembolism (CME) results from the disruption of unstable atherosclerotic plaques or the occlusion of distal coronary arteries by microthrombi, atherosclerotic debris, or other particulate matter. This condition often occurs after percutaneous coronary intervention (PCI). It may cause coronary slow-flow or no-reflow phenomena, which can trigger dangerous arrhythmias and localized myocardial systolic dysfunction. Moreover, CME is a strong independent predictor of poor long-term outcomes and major adverse cardiovascular events (1-3). Routine use of interventional protection devices has not demonstrated significant clinical benefits in patient outcomes, and current management of CME continues to depend on statins, platelet inhibitors, and vasodilators (4). Therefore, novel therapeutic approaches for CME prevention and treatment are urgently needed.

Ferroptosis, a recently discovered form of programmed cell death, involves iron-dependent accumulation of lipid peroxides within cells (5). This process has been implicated in multiple cardiovascular pathologies (6-8). During ischemia, the myocardium accumulates pathological iron and ROS, leading to detrimental changes in membrane lipids—the hallmark of ferroptosis. Ferroptotic myocardium exhibits increased oxidative stress, elevated endoplasmic reticulum stress, excessive iron overload, and impaired mitochondrial function (9). Studies have demonstrated that oxidative stress, inflammation, and ferroptosis contribute to myocardial injury after CME (10, 11). Notably, atorvastatin has been shown to reduce CME-mediated ferroptosis-induced myocardial injury via the Hif1α/Ptgs2 pathway. These findings establish ferroptosis as a potential therapeutic target for alleviating CME-induced myocardial injury (12).

Quercetin, a flavonoid found in apples, onions, tea,

***Corresponding author:** Lang Li. Department of Cardiology, The First Affiliated Hospital of Guangxi Medical University, Guangxi Cardiovascular Institute, Nanning 530021, Guangxi, China. Tel/ Fax: +86-13607881856 , Email: drlilang@gxmu.edu.cn

red wine, and berries, exhibits a broad spectrum of beneficial effects, including cardiovascular protection, anti-inflammatory effects, anti-cancer properties, and anti-ulcer activity (13). Nrf2, a key transcription factor, regulates antioxidant and anti-inflammatory responses, thereby protecting cells from oxidative stress and inflammation-mediated damage (14). Quercetin modulates ferroptosis through the SIRT1/Nrf2/HO-1 pathway, reducing cartilage degradation in rat models of osteoarthritis (15). Additionally, Quercetin has been shown to ameliorate diabetic nephropathy by inhibiting ferroptosis and regulating Nrf2 in streptozotocin-induced diabetic rats (16). While these benefits are established, it remains unknown whether Quercetin protects against CME-induced myocardial damage via Nrf2 activation. Therefore, this study aims to investigate whether quercetin administration can mitigate CME-induced myocardial damage and suppress ferroptosis in cardiomyocytes from CME rats by activating the Nrf2/HO-1 signaling pathway.

Materials and Methods

Animal grouping and model construction

Twenty-eight male Sprague-Dawley (SD) rats, 8 weeks old and weighing 200-250 g, were obtained from the Laboratory Animal Center of Guangxi Medical University (specific pathogen-free grade). The rats were randomly assigned to four experimental groups: Sham, CME, CME+Quercetin (Que), and CME+Quercetin+ML385 (Que+ML385), with 7 rats per group. All animals were maintained under controlled environmental conditions at 25 ˚C with a 12-hour light-dark cycle and had free access to food and water.

The CME model was established following previously published protocols (6). Briefly, rats were anesthetized by intraperitoneal injection of sodium pentobarbital (40 mg/kg). After standard aseptic preparation, mechanical ventilation was initiated with settings of 70 breaths/min and 7 ml tidal volume to support respiration, and a surgical incision was made along the left sternal border to expose the ascending aorta. The aorta was temporarily occluded using a vascular clamp, and 0.2 ml of microsphere suspension (8,000 particles, 42 μm diameter; Polysciences Inc., USA) was injected into the left ventricular apex. The vascular clamp was removed after twelve seconds. Sham-operated animals received an equivalent volume of normal saline using the identical procedure.

In the Que group, rats were pretreated with quercetin (250 mg/kg/day) via oral gavage for 7 consecutive days, including the day of model induction. The Que+ML385 group received the same quercetin pretreatment plus an additional intraperitoneal injection of ML385 (30 mg/kg) 2 hr before model establishment.

The experimental protocol was approved by the Animal Research Ethics Committee of Guangxi Medical University (application number: 202401013) and complied with the National Institutes of Health guidelines for laboratory animals.

Heart echocardiography

Cardiac function was assessed six hours after surgery. Under anesthesia, myocardial performance parameters were evaluated using a high-frequency 12 MHz transducer integrated with the MyLabSix echocardiography platform (Esaote, Italy). Echocardiography data are obtained from M-shaped images of the short-axis section beside the sternum at the level of the papillary muscle. Measurements included left ventricular ejection fraction (LVEF), fractional shortening (FS), left ventricular end-diastolic diameter (LVEDD), and end-systolic diameters (LVESD). Measurements were performed by an echocardiographer blinded to treatment groups to ensure objective data collection. Parameters represent the mean of three consecutive cardiac cycles to improve measurement reliability.

Sample collection

After assessing cardiac function, we euthanized the experimental rats by intraperitoneal injection of a lethal dose of pentobarbital sodium, then collected blood samples from the abdominal aorta and centrifuged them to isolate serum for biochemical analysis. After excising the cardiac tissue, we perfused it with cold saline, removed the auricular and atrial components, and rapidly froze the ventricular apex in liquid nitrogen. We stored the cryopreserved specimens at -80 ˚C for subsequent qRT-PCR and western blot analyses. We fixed the remaining cardiac tissue in 4% neutral buffered formaldehyde for 12 hr before embedding it in paraffin. Serial sections of 4-μm thickness were prepared for comprehensive histopathological evaluation and immunofluorescence studies.

Serum markers

Commercial kits from Solarbio were used to measure serum concentrations of cTnI, CK-MB, Fe^{2+}, GSH, and MDA, following the manufacturer's instructions.

HE and Heidenhain's iron hematoxylin staining

HE and Heidenhain's iron hematoxylin staining were used to assess myocardial microinfarction areas and histomorphological changes. Heidenhain's iron hematoxylin stain provides superior contrast for detecting early myocardial ischemia. In normal myocardial tissue, cardiomyocyte cytoplasm stains red with distinct black nuclei, whereas ischemic cardiomyocytes and erythrocytes exhibit characteristic black staining (17). Heidenhain's iron hematoxylin staining has been widely used to identify early ischemic myocardial injury and microinfarction after CME (18, 19). Staining was observed under a ZEISS Axio Imager A2 microscope (Carl Zeiss AG, Germany). For each section, five representative images from different fields were systematically acquired, and the infarct area was measured using ImageJ software. The percentage of the microinfarct area was then calculated. Image acquisition and data analysis were performed by an independent researcher who was unaware of the grouping.

Immunofluorescence staining

To examine the subcellular localization and relative abundance of ACSL4, Ferritin, and GPX4 in rat cardiac tissue, we performed immunofluorescence analysis. Tissue sections were incubated with the following primary antibodies: anti-ACSL4 (1:500; Abcam, USA), anti-Ferritin (1:500; Bioss, China), and anti-GPX4 (1:500; Abcam, USA) at 4 ˚C overnight, then incubated with fluorescently labeled secondary antibody (1:500; Abcam, USA) protected from light for 60 min. Nuclear counterstaining with DAPI was performed, with all procedures strictly following

manufacturers' protocols. Fluorescence imaging was performed with an Olympus BX53F microscope (Japan), and fluorescence intensity was quantified using ImageJ.

Quantitative real-time PCR

Total RNA was extracted using Trizol reagent (Invitrogen) following the manufacturer's standard protocol, including phase separation, RNA precipitation, and washing. RNA concentration and purity (A260/A280 ratio >1.8) were measured with a NanoDrop 2000 spectrophotometer (Thermo Fisher Scientific). We synthesized complementary DNA with a commercial reverse transcription kit (Takara) and performed quantitative real-time PCR on an ABI 7500 platform (Applied Biosystems) using SYBR Green I master mix (ACE Biotechnology). All qPCR reactions, performed in technical triplicate, were normalized to the housekeeping gene GAPDH. We quantified relative gene expression using the 2–ΔΔCt method for comparative threshold cycle analysis. Primer sequences are listed in Table 1.

Western blotting

Cardiac tissues were homogenized in RIPA buffer supplemented with protease inhibitors using a mechanical tissue homogenizer. Following centrifugation at 12,000×g for 15 min at 4 ˚C, the protein-containing supernatant was collected, and protein concentration was determined via the bicinchoninic acid (BCA) assay. Equal amounts of protein were loaded for SDS-PAGE. For immunoblotting, samples were separated on 12% SDS-polyacrylamide gels and then transferred by electrotransfer onto polyvinylidene fluoride (PVDF) membranes. Membranes were blocked to prevent nonspecific binding with 5% non-fat dry milk in Tris-buffered saline containing 0.1% Tween-20 (TBST) for 60 min at room temperature. After blocking, membranes were incubated with primary antibodies targeting key ferroptosis-related proteins: ACSL4 (Abcam, USA; 1:2000), FTH1 (Bioss, China; 1:2000), GPX4 (Abcam, USA; 1:2000), Nrf2 (Abcam, USA; 1:2000), and HO-1 (Bioss, China; 1:2000) for 16 hr at 4 ˚C. After extensive washing with TBST, membranes were incubated for 60 min at room temperature with species-matched fluorescent secondary antibodies (1:10,000 dilution). Protein signals were detected using enhanced chemiluminescence reagents and captured using the Pierce detection system. Band intensities were quantified using ImageJ software (version 1.80) for densitometric analysis.

Table 1. Primer sequences of the target genes used in qRT-PCR analysis

Gene	primer sequences
Nrf2 F	5′-CTGCTCCGACTAGCCATTGAC-3
Nrf2 R	5′-TGTCTTGCCTCCAAAGGATGTC-3′
HO-1 F	5′-CACGCATATACCCGCTACCT-3′
HO-1 R	5′-AAGGCGGTCTTAGCCTCTTC-3′
ACSL4 F	5′-CAGGGCTATGGGCTGACAGAAT-3′
ACSL4 R	5′-TGAACTGTATAACCACCTTCCTGC-3′
GPX4 F	5'-TGAGGCAAAACCGACGTAAACT-3'
GPX4 R	5'-TTGATTACTTCCTGGCTCCTGC-3'
GAPDH F	5-TGGAGAAACCTGCCAAGTATGATG-3'
GAPDH R	5'-TATCCTTGCTGGGCTGGGTG-3'

Nrf2: Nuclear factor erythroid 2-related factor 2; HO-1: Heme oxygenase-1; ACSL4:Acyl-CoA synthetase long-chain family member 4; Gpx4: Glutathione peroxidase 4; GAPDH: Glyceraldehyde-3-phosphate dehydrogenase

Statistical analysis

Statistical analyses were performed using SPSS 25.0 (IBM Corp.), with quantitative data presented as mean±standard deviation. We used the Shapiro-Wilk test to assess whether the data were normally distributed, and Levene's test to assess homogeneity of variance. If the data were normally distributed and had homogeneity of variance, we used one-way ANOVA, followed by Fisher's LSD *post hoc* test to compare differences between groups. If the variances were unequal, we used Dunnett's T3 *post hoc* test to compare differences between groups. The statistical significance level was set at $P<0.05$.

Results

Quercetin improves cardiac function after CME in rats

Cardiac function was assessed by echocardiography. Compared with the Sham group, rats in the CME group exhibited significantly reduced LVEF and LVFS, accompanied by a marked increase in LVESD, indicating impaired left ventricular systolic function. Quercetin pretreatment significantly attenuated these functional abnormalities, as evidenced by increased LVEF and LVFS and decreased LVESD compared with the CME group. Notably, concurrent administration of ML385 abolished the cardioprotective benefits of quercetin. Comprehensive echocardiographic data for all experimental groups are presented in Figure 1.

Effects of quercetin on myocardial injury and ferroptosis marker levels

Serum levels of cTnI and CK-MB reflect myocardial injury in rats following CME. Additionally, markers such as MDA, GSH, and Fe^{2+} are closely associated with ferroptosis and redox reactions. Results showed significant increases in cTnI, CK-MB, MDA, and Fe^{2+} levels in the CME group versus Sham controls. Conversely, GSH levels were substantially reduced. Importantly, quercetin pretreatment significantly attenuated CME-induced myocardial injury. The Que group showed decreased serum levels of cTnI, CK-MB, MDA, and Fe^{2+} but increased GSH compared to the CME group. However, co-administration of ML385 partially reversed quercetin's protective effects (Figure 2). These findings demonstrate that quercetin mitigates myocardial damage and suppresses ferroptosis in CME rats.

Quercetin reduces microinfarct size in CME rats

HE staining revealed no microembolic lesions or myocardial infarction in the Sham group, with myocardial fibers intact and neatly arranged. In contrast, intravascular microemboli were observed in the other groups. In these groups, myocardial fibers were disorganized around the microemboli, myocardial cell nuclei showed dissolution or disappearance, and leukocyte infiltration with erythrocyte exudation was observed. Additionally, Heidenhain's iron hematoxylin staining showed that the myocardial infarction area in the Sham, CME, Que, and Que+ML385 groups was 1.74±0.47%, 17.95±3.87%, 10.28±1.81%, and 17.12±0.48%,

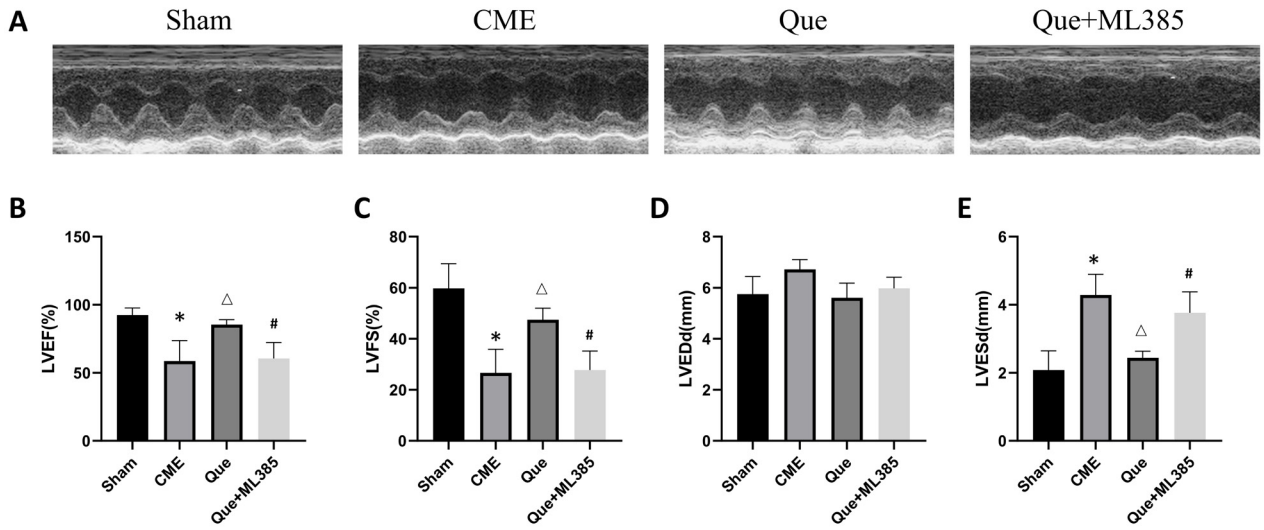

Figure 1. Quercetin improves cardiac function in rats after CME
(A) Representative echocardiograms of each group. (B-E) LVEF, LVFS, LVEDd, and LVESd in each group of rats. The data were analyzed using one-way ANOVA with *post hoc* Fisher's LSD test and presented as mean±SD (n = 7). $^{*}P<0.05$ vs Sham group; $^{\triangle}P<0.05$ vs CME group; $^{\#}P<0.05$ vs Que group
LVEF: Left ventricular ejection fraction; LVFS: left ventricular fractional shortening; LVEDd: left ventricular end-diastolic diameter; LVESd: left ventricular end-systolic diameters

respectively. Compared to the CME group, the infarct size in the Que group was significantly reduced, indicating that quercetin pretreatment reduces infarct size in CME-induced myocardial injury while decreasing peripheral myocardial edema and inflammatory cell infiltration. However, ML385 co-administration significantly reversed these beneficial effects (Figure 3).

Quercetin pretreatment reduces the levels. Figures

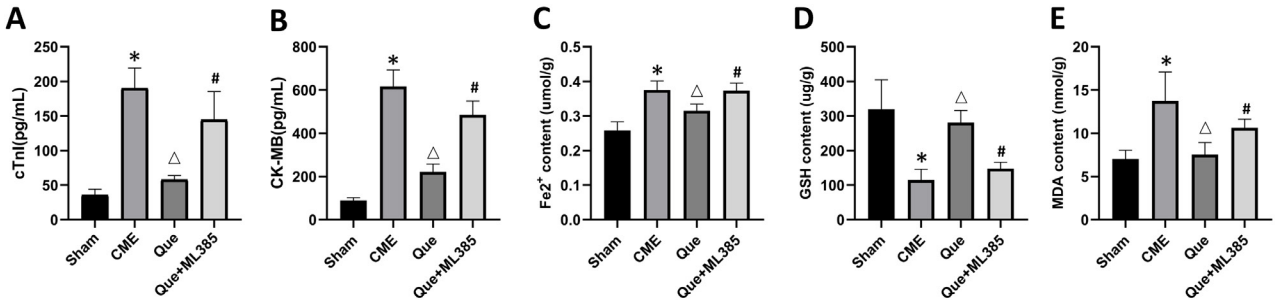

Figure 2. Quercetin reduces myocardial injury and ferroptosis marker levels in rats
(A-E) Levels of serum cTnI, CK-MB, Fe2+, GSH, and MDA. Data are presented as the mean±SD (n=6). Statistical analyses for Figure 2A, Figure 2D, and Figure 2E were performed using one-way ANOVA followed by Dunnett's T3 *post hoc* test, while Figure 2B and Figure 2C were analyzed using one-way ANOVA followed by Fisher's LSD *post hoc* test. $^{*}P<0.05$ vs Sham group; $^{\triangle}P<0.05$ vs CME group; $^{\#}P<0.05$ vs Que group
cTnI: Cardiac troponin I; CK-MB: Creatine kinase MB isoenzyme; GSH: Glutathione; MDA: Malondialdehyde

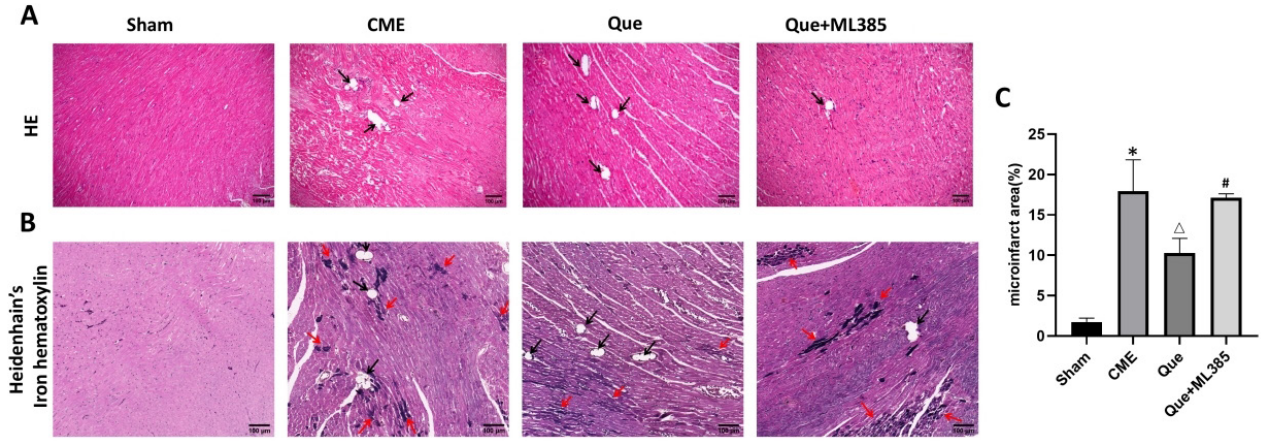

Figure 3. Hematoxylin and Eosin (HE) and Heidenhain iron hematoxylin staining of rat tissue
(A) HE staining. Microspheres with inflammatory cell infiltration were observed in the CME, Que, and Que+ML385 groups, but not in the sham surgery group. Black arrows indicate microspheres (×100 magnification; scale bar=100μm)(n=3). (B) Heidenhain iron hematoxylin staining. Ischemic myocardium is prominently displayed in brown-black. Red arrows indicate the area of microinfarction. (C) The microinfarct size in each group. The data were analyzed using one-way ANOVA with *post hoc* Fisher's LSD test and presented as mean±SD. $^{*}P<0.05$ vs Sham group; $^{\triangle}P<0.05$ vs CME group; $^{\#}P<0.05$ vs Que group
HE: Hematoxylin and eosin staining

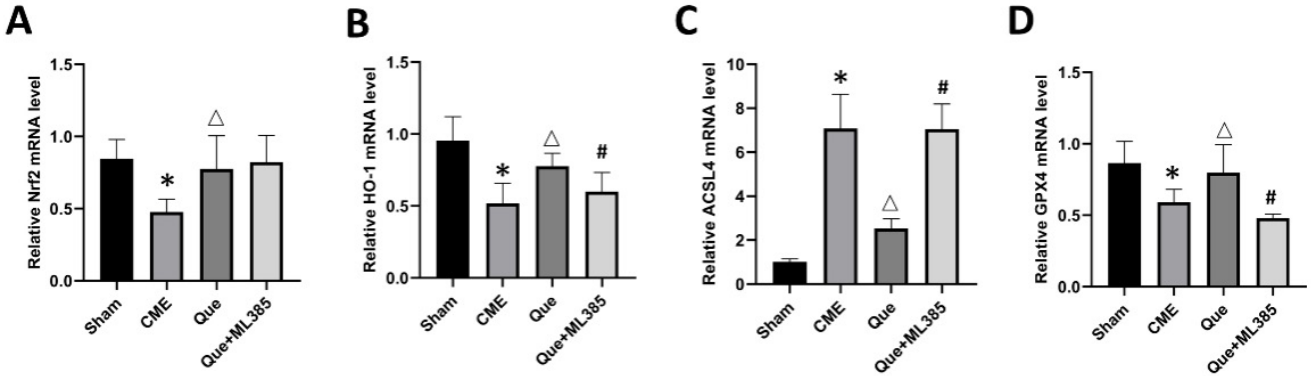

Figure 4. (A-D) Changes in mRNA expression levels of Nrf2, HO-1, ACSL4, and Gpx4 across rat groups
Data are presented as mean±SD (n=4). Statistical analyses for Figures 4A and 4C were performed using one-way ANOVA with Dunnett's T3 *post hoc* test, whereas Figures 4B and 4D were analyzed using one-way ANOVA with Fisher's LSD *post hoc* test. $^{*}P<0.05$ vs Sham group; $^{\triangle}P<0.05$ vs CME group; $^{\#}P<0.05$ vs Que group
Nrf2: Nuclear factor erythroid 2-related factor 2; HO-1: Heme oxygenase-1; ACSL4: Acyl-CoA synthetase long-chain family member 4; Gpx4: Glutathione peroxidase 4

4A and 4C were performed using one-way ANOVA with Dunnett's T3 *post hoc* test, whereas Figures 4B and PCR for mRNA and western blot for protein analysis were performed. We measured ACSL4 and GPX4 expression in rat heart tissue. The CME group showed significantly increased ACSL4 and decreased GPX4 levels ($P<0.05$). Quercetin treatment resulted in a pronounced reduction in ACSL4 expression and a corresponding increase in GPX4 levels. Combined quercetin and ML385 treatment further altered the expression patterns, decreasing ACSL4 and increasing GPX4 and ferritin levels (Figures 4 and 5). Immunohistochemistry (Figures 6 and 7) showed results consistent with qRT-PCR and western blot. The results indicate that quercetin pretreatment can effectively reduce the levels of ferroptosis-related marker proteins, suggesting that quercetin may alleviate CME-induced ferroptosis in cardiomyocytes.

Quercetin pretreatment activates the Nrf2/HO-1 signaling pathway

Both qRT-PCR and western blot analyses showed that Nrf2 and HO-1 expression levels were significantly decreased in the CME group. In contrast, Nrf2 and HO-1 expression were markedly increased in the Que group compared with the CME group ($P<0.05$)(Figures 4 and 5). These findings suggest quercetin pretreatment may attenuate CME-induced cardiomyocyte ferroptosis by activating the Nrf2/HO-1 signaling pathway.

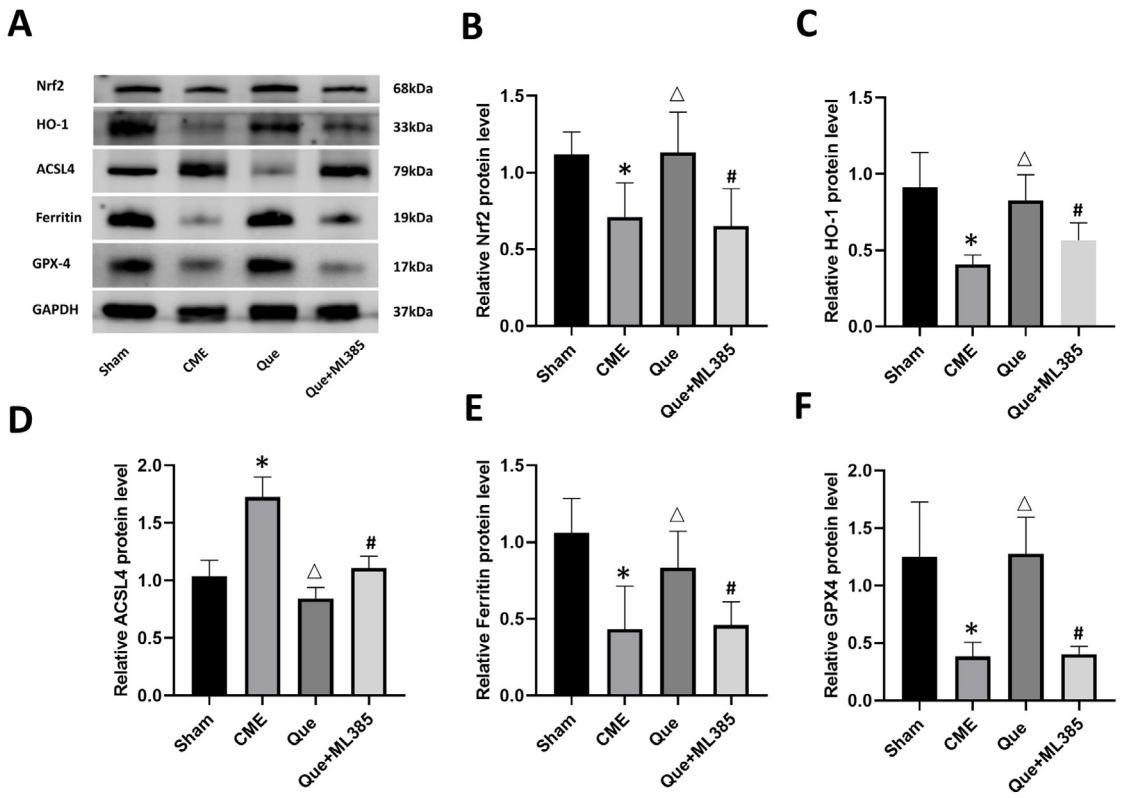

Figure 5. Quercetin inhibits cardiomyocyte ferroptosis through the Nrf2/HO-1 signaling pathway in rats
(A-F): Changes of relative expression levels of Nrf2, HO-1, ACSL4, Ferritin, and Gpx4 proteins in each group.The data were analyzed using one-way ANOVA with *post hoc* Fisher's LSD test and presented as mean±SD (n=4). $^{*}P<0.05$ vs Sham group; $^{\triangle}P<0.05$ vs CME group; $^{\#}P<0.05$ vs Que group
Nrf2: Nuclear factor erythroid 2-related factor 2; HO-1: Heme oxygenase-1; ACSL4: Acyl-CoA synthetase long-chain family member 4; Gpx4: Glutathione peroxidase 4

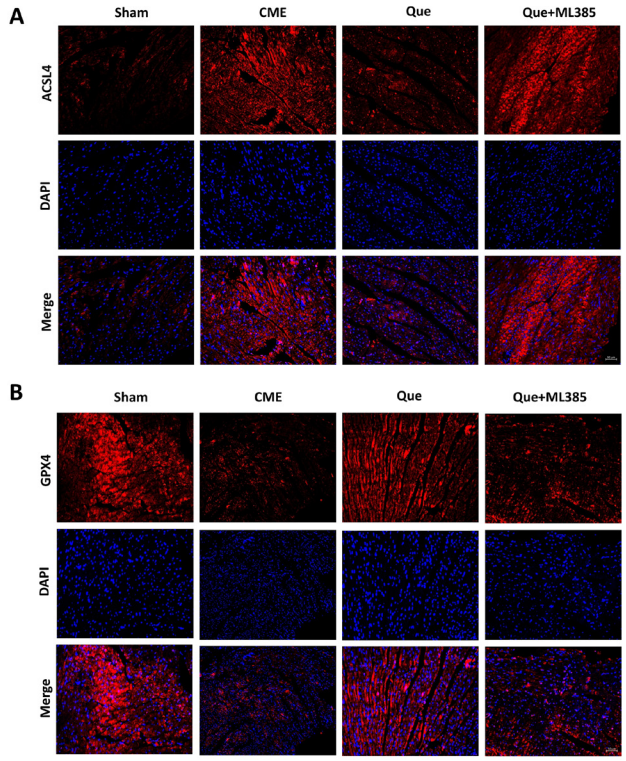

Figure 6. Subcellular localization and relative abundance of ACSL4 and GPX4 in rat myocardial tissue for each group (n=3)
(A) Representative immunofluorescence images of ACSL4. (B) Representative immunofluorescence images of GPX4. Magnification,×200; Scale bar =100 μm
ACSL4: Acyl-CoA synthetase long-chain family member 4; Gpx4: Glutathione peroxidase 4

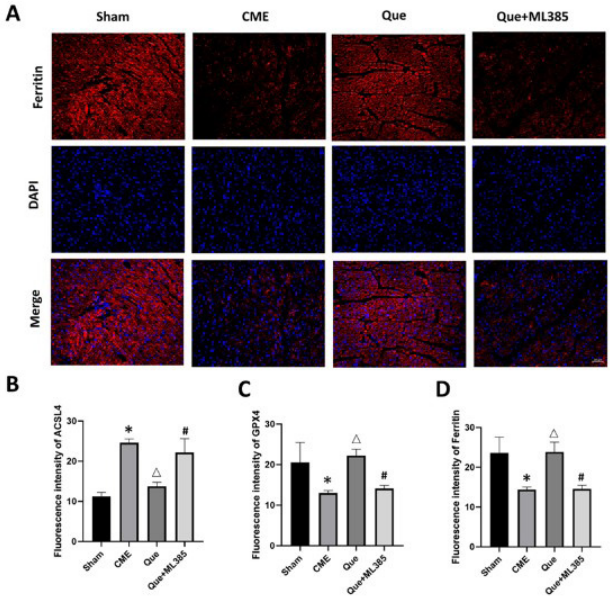

Figure 7. Immunofluorescence images of Ferritin in rat myocardial tissue for each group (n=3)
(A) Representative immunofluorescence images of Ferritin. Magnification,×200; Scale bar =100 μm. (B-D): The fluorescence intensity of ACSL4, Ferritin, and Gpx4 for each group. The data were analyzed using one-way ANOVA with *post hoc* Fisher's LSD test and presented as mean±SD (n=3). $^{*}P<0.05$ vs Sham group; $^{\triangle}P<0.05$ vs CME group; $^{\#}P<0.05$ vs Que group
ACSL4: Acyl-CoA synthetase long-chain family member 4; Gpx4: Glutathione peroxidase 4

Discussion

In this study, we successfully established a rat model to investigate coronary microembolization (CME). Our results showed that CME damage increases levels of myocardial oxidative and ferroptosis-related biochemical markers. Pretreatment with quercetin may attenuate myocardial ferroptosis by activating the Nrf2/HO-1 pathway, thereby reducing cardiomyocyte damage and improving cardiac function in rats.

The pathophysiological mechanisms of CME involve multiple processes, including inflammation, oxidative stress, and apoptosis (10, 18, 20, 21). Ferroptosis, a form of regulated cell death, contributes to cardiovascular disease progression and is a therapeutic target for myocardial injury, cardiomyopathy, cardiac stress injury, and ischemia/reperfusion injury (22). For example, Yang *et al.* reported that ferroptosis is activated in mice with acute myocardial infarction, and its inhibition significantly improved cardiac function while reducing myocardial inflammation and fibrosis (23). Similarly, Tan *et al.* showed that ferroptosis occurs in both *in vitro* and *in vivo* models of myocardial I/R injury, and that TMZ attenuated I/R-induced ferroptosis by activating the Sirt3-Nrf2/GPX4/SLC7A11 pathway, thereby decreasing myocardial damage (24). Furthermore, Wu *et al.* found that LBH-CRYAB signaling was activated in cardiomyocytes during I/R injury, and that LBH overexpression inhibited both apoptosis and ferroptosis, enhancing the heart's protective response to I/R injury (25).

Ferroptosis activation after CME is a key mechanism contributing to CME-induced myocardial injury, and its inhibition holds therapeutic potential for alleviating cardiomyocyte damage in CME (12). Ferroptosis is an iron-dependent, lipid peroxide-driven programmed cell death pathway. Mechanistically, ACSL4 is a lipid metabolism enzyme that promotes the generation of lipid peroxides, thereby promoting ferroptosis. However, SLC7A11 transports cysteine into the cell, where cysteine is the precursor of glutathione (GSH), the main intracellular antioxidant. GSH plays a critical role in ferroptosis. It can reduce lipid peroxides to normal lipids via GPX4, preventing the accumulation of lipid peroxides and thus inhibiting the occurrence of ferroptosis. Therefore, the SLC7A11/GSH/GPX4 pathway has been established as one of the key mechanisms for protecting cells from ferroptosis(26). In our research, we used molecular biology techniques to measure the levels of biochemical markers related to cardiomyocyte ferroptosis after CME. Quercetin pretreatment markedly reduced the expression of ACSL4, a ferroptosis-associated protein, while increasing levels of anti-ferroptosis markers, including GSH, ferritin, and GPX4. These findings indicate quercetin may protect the heart by preventing CME-induced cardiomyocyte ferroptosis.

Quercetin, a prominent flavonoid compound first isolated in the early 20th century, has emerged as a molecule of significant pharmacological interest due to its multifaceted biological effects. Extensive research has documented its wide-ranging therapeutic properties, including immune response modulation, antimicrobial activity, anticancer potential, neuroprotection, allergy suppression, and potent antioxidative and anti-inflammatory actions (13, 27-29). In the cardiovascular domain, quercetin has demonstrated remarkable cardioprotective capabilities through multiple mechanisms. Notably, it modulates cardiac autophagy and prevents programmed cell death in diabetic cardiac tissue by influencing the AMPK/mTOR axis, leading to improved

myocardial performance (30). Furthermore, quercetin exhibits protective effects against ischemia-reperfusion-induced cardiac injury by maintaining mitochondrial homeostasis through the DNA-PKcs-SIRT5 pathway and mitigating oxidative damage in cardiomyocytes (31). In the *in vitro* human coronary endothelial cell hypoxia/reoxygenation (H/R) model, quercetin up-regulated the expression of Nrf2 and HO-1, reduced MDA levels, and increased SOD and CAT activities, thereby alleviating H/R-induced oxidative stress, mitochondrial damage, and apoptosis (32). Our experiments showed that quercetin pretreatment produced two key benefits: (1) suppression of oxidative stress and (2) attenuation of ferroptosis in cardiomyocytes. These combined effects led to reduced myocardial damage and improved cardiac function in our coronary microembolization models. These observations position quercetin as a promising therapeutic candidate for coronary microembolization syndrome.

The Nrf2/HO-1 signaling axis represents a critical defensive mechanism against cardiovascular pathologies, with its activity intimately linked to oxidative stress regulation and ferroptosis prevention (33, 34). Previous investigations have established that pharmacological activation of this pathway can counteract doxorubicin-induced cardiotoxicity by suppressing ferroptotic processes in myocardial cells (35). Similarly, isoglycyrrhizin has been shown to confer myocardial protection through Nrf2/HO-1-mediated up-regulation of the SLC7A11/GPX4 antioxidant system (36). Quercetin can also exert its antioxidant effect by activating the Nrf2/HO-1 signaling pathway in various disease models. In the diabetic nephropathy model, quercetin inhibits ferroptosis by activating the Nrf2/HO-1 signaling pathway, thereby alleviating diabetic kidney injury (37). In rat cerebral ischemia models, quercetin attenuates cerebral ischemic injury by inhibiting ferroptosis via the Nrf2/HO-1 signaling pathway (38). Our research group has previously documented the involvement of this pathway in coronary microembolization pathology, demonstrating its capacity to reduce cardiomyocyte apoptosis and limit myocardial injury (39-41). In the current investigation, we observed marked down-regulation of both transcriptional and translational expression of Nrf2 and HO-1 in coronary microembolization subjects. Quercetin intervention effectively restored the expression of these protective factors, consequently inhibiting ferroptotic processes and improving cardiac outcomes. The reversal of quercetin's beneficial effects upon administration of the Nrf2 antagonist ML385, along with corroborative immunofluorescence findings, provides compelling evidence for the central role of the Nrf2/HO-1 pathway in mediating quercetin's cardioprotective actions in coronary microembolization.

These encouraging results have several limitations. The study examined acute myocardial injury in coronary microembolization models but did not assess long-term therapeutic outcomes. Furthermore, the study used a relatively small animal cohort. Future research should use primary cardiomyocyte cultures for *in vitro* analysis. This study detected changes only in oxidative-related myocardial injury and in ferroptosis-related biochemical markers. Future studies need to employ direct ferroptosis detection methods (such as aldehyde oxidation measurements and transmission electron microscopy of mitochondrial morphology) to confirm cellular ferroptosis. We need to fully elucidate the molecular mechanism of quercetin and assess whether quercetin can provide a sustained therapeutic effect on CME.

Conclusion

In summary, as this study reveals, Quercetin may inhibit ferroptosis in cardiomyocytes by activating the Nrf2/HO-1 signaling pathway, thereby improving CME-related cardiac dysfunction and reducing myocardial injury. Overall, quercetin is a promising treatment for CME that deserves further research.

Acknowledgment

None.

Funding

This research did not receive any specific grant from funding agencies in the public, commercial, or not-for-profit sectors.

Authors' Contributions

J H and L L designed the experiments; J H and Z T performed the experiments and collected data; J H, G T, and J N analyzed and interpreted the results; J H drafted the manuscript, prepared the visualization, and edited the article. L L supervised, directed, and managed the study; J H, Z T, J N, G T, X F, and L L gave final approval of the version to be published.

Conflicts of Interest

The authors declare no conflicts of interest.

Declaration

We have not used any AI tools or technologies to prepare this manuscript.

References

1. Heusch G, Skyschally A, Kleinbongard P. Coronary microembolization and microvascular dysfunction. Int J Cardiol 2018; 258: 17–23.
2. Scarpone M, Cenko E, Manfrini O. Coronary no-reflow phenomenon in clinical practice. Curr Pharm Des 2018; 24: 2927-2933.
3. Skyschally A, Leineweber K, Gres P, Haude M, Erbel R, Heusch G. Coronary microembolization. Basic Res Cardiol 2006; 101: 373-382.
4. Kleinbongard P, Heusch G. A fresh look at coronary microembolization. Nat Rev Cardiol 2022; 19: 265-280.
5. Zheng J, Conrad M. The metabolic underpinnings of ferroptosis. Cell Metab 2020; 32: 920-937.
6. Wang H, Huang Z, Du C, Dong M. Iron dysregulation in cardiovascular diseases. Rev Cardiovasc Med 2024; 25: 16.
7. Chen W, Zhang Y, Wang Z, Tan M, Lin J, Qian X, *et al.* Dapagliflozin alleviates myocardial ischemia/reperfusion injury by reducing ferroptosis via MAPK signaling inhibition. Front Pharmacol 2023; 14: 1078205.
8. Wang X, Chen X, Zhou W, Men H, Bao T, Sun Y, *et al.* Ferroptosis is essential for diabetic cardiomyopathy and is prevented by sulforaphane via AMPK/NRF2 pathways. Acta Pharm Sin B 2022; 12: 708–722.
9. Luan X, Chen P, Miao L, Yuan X, Yu C, Di G. Ferroptosis in organ ischemia-reperfusion injuries: recent advancements and strategies. Mol Cell Biochem 2024; 480: 19-41.
10. Zhou Y, Long MY, Chen ZQ, Huang JW, Qin ZB, Li L. Downregulation of miR-181a-5p alleviates oxidative stress and inflammation in coronary microembolization-induced myocardial

damage by directly targeting XIAP. J Geriatr Cardiol 2021; 18: 426-439.
11. Xie J, Mo B, Lin Y, Liu G, Nong Q, Wu B, *et al.* Human urinary kallidinogenase pretreatment inhibits myocardial inflammation and apoptosis after coronary microembolization by activating PI3K/Akt/FoxO1 axis. Front Biosci (Landmark Ed) 2022; 27: 298.
12. Liu T, Shu J, Liu Y, Xie J, Li T, Li H, *et al.* Atorvastatin attenuates ferroptosis-dependent myocardial injury and inflammation following coronary microembolization via the Hif1a/Ptgs2 pathway. Front Pharmacol 2022; 13: 1057583.
13. Vollmannová A, Bojňanská T, Musilová J, Lidiková J, Cifrová M. Quercetin as one of the most abundant represented biological valuable plant components with remarkable chemoprotective effects - A review. Heliyon 2024; 10: e33342.
14. Luchkova A, Mata A, Cadenas S. Nrf2 as a regulator of energy metabolism and mitochondrial function. FEBS Lett 2024; 598: 2092-2105.
15. Ruan H, Zhu T, Wang T, Guo Y, Liu Y, Zheng J. Quercetin modulates ferroptosis via the SIRT1/Nrf-2/HO-1 pathway and attenuates cartilage destruction in an osteoarthritis rat model. Int J Mol Sci 2024; 25: 7461.
16. Zhang L, Wang X, Chang L, Ren Y, Sui M, Fu Y, *et al.* Quercetin improves diabetic kidney disease by inhibiting ferroptosis and regulating the Nrf2 in streptozotocin-induced diabetic rats. Ren Fail 2024; 46: 2327495.
17. Ferris JA, Friesen JM. Definitions of ischaemia, infarction and necrosis. Forensic Sci Int 1979; 13: 253–259.
18. Chen A, Chen Z, Zhou Y, Wu Y, Xia Y, Lu D, *et al.* Rosuvastatin protects against coronary microembolization-induced cardiac injury via inhibiting NLRP3 inflammasome activation. Cell Death Dis 2021; 12: 78.
19. Yang T, Wu X, Wang X. HMGB1 regulates autophagy via TLR4/NF-κB signaling pathway in myocardial injury induced by coronary microembolization. Eur J Med Res 2025; 30: 943.
20. Li T, Chen Z, Zhou Y, Li H, Xie J, Li L. Resveratrol pretreatment inhibits myocardial apoptosis in rats following coronary microembolization via inducing the PI3K/Akt/GSK-3β signaling cascade. Drug Des Devel Ther 2021; 15: 3821–3834.
21. Li H, Yang H, Qin Z, Wang Q, Li L. Colchicine ameliorates myocardial injury induced by coronary microembolization through suppressing pyroptosis via the AMPK/SIRT1/NLRP3 signaling pathway. BMC Cardiovasc Disord 2024; 24: 23.
22. Ryabov VV, Maslov LN, Vyshlov EV, Mukhomedzyanov AV, Kilin M, Gusakova SV, *et al.* Ferroptosis, a regulated form of cell death, as a target for the development of novel drugs preventing ischemia/reperfusion of cardiac injury, cardiomyopathy and stress-induced cardiac injury. Int J Mol Sci 2024; 25: 897.
23. Yang C, Guo W, He R, Meng X, Fu J, Lu Y. Dietary capsaicin attenuates cardiac injury after myocardial infarction in type 2 diabetic mice by inhibiting ferroptosis through activation of TRPV1 and Nrf2/HMOX1 pathway. Int Immunopharmacol 2024; 140: 112852.
24. Tan M, Yin Y, Chen W, Zhang J, Jin Y, Zhang Y, *et al.* Trimetazidine attenuates Ischemia/Reperfusion-Induced myocardial ferroptosis by modulating the Sirt3/Nrf2-GSH system and reducing Oxidative/Nitrative stress. Biochem Pharmacol 2024; 229: 116479.
25. Wu A, Zhong C, Song X, Yuan W, Tang M, Shu T, *et al.* The activation of LBH-CRYAB signaling promotes cardiac protection against I/R injury by inhibiting apoptosis and ferroptosis. iScience 2024; 27: 109510.
26. Chen G, Luo S, Guo H, Lin J, Xu S. Licochalcone A alleviates ferroptosis in doxorubicin-induced cardiotoxicity via the PI3K/AKT/MDM2/p53 pathway. Naunyn Schmiedebergs Arch Pharmacol 2024; 397: 4247–4262.
27. Shorobi FM, Nisa FY, Saha S, Chowdhury MAH, Srisuphanunt M, Hossain KH, *et al.* Quercetin: A functional food-flavonoid incredibly attenuates emerging and re-emerging viral infections through immunomodulatory actions. Molecules 2023; 28: 938.
28. Grewal AK, Singh TG, Sharma D, Sharma V, Singh M, Rahman MH, *et al.* Mechanistic insights and perspectives involved in neuroprotective action of quercetin. Biomed Pharmacother 2021; 140: 111729.
29. Onaolapo AY, Ojo FO, Onaolapo OJ. Biflavonoid quercetin protects against cyclophosphamide-induced organ toxicities via modulation of inflammatory cytokines, brain neurotransmitters, and astrocyte immunoreactivity. Food Chem Toxicol 2023; 178: 113879.
30. Chen YF, Qiu Q, Wang L, Li XR, Zhou S, Wang H, *et al.* Quercetin ameliorates myocardial injury in diabetic rats by regulating autophagy and apoptosis through AMPK/mTOR signaling pathway. Am J Chin Med 2024; 52: 841–864.
31. Chang X, Zhang Q, Huang Y, Liu J, Wang Y, Guan X, *et al.* Quercetin inhibits necroptosis in cardiomyocytes after ischemia-reperfusion via DNA-PKcs-SIRT5-orchestrated mitochondrial quality control. Phytother Res 2024; 38: 2496–2517.
32. Song J, Li S, Zhang B, Wu J, Zhong A. Quercetin protects human coronary artery endothelial cells against hypoxia/reoxygenation-induced mitochondrial apoptosis via the Nrf2/HO-1 axis. Biomed Res 2024; 45: 197–207.
33. Sun YY, Zhu HJ, Zhao RY, Zhou SY, Wang MQ, Yang Y, *et al.* Remote ischemic conditioning attenuates oxidative stress and inflammation via the Nrf2/HO-1 pathway in MCAO mice. Redox Biol 2023; 66: 102852.
34. Wu S, Zhu J, Wu G, Hu Z, Ying P, Bao Z, *et al.* 6-Gingerol alleviates Ferroptosis and inflammation of diabetic cardiomyopathy via the Nrf2/HO-1 pathway. Oxid Med Cell Longev 2022; 2022: 3027514.
35. Xue S, Chen H, Zhang J, Tian R, Xie C, Sun Q, *et al.* Qishen granule alleviates doxorubicin-induced cardiotoxicity by suppressing ferroptosis via nuclear erythroid factor 2-related factor 2 (Nrf2) pathway. J Ethnopharmacol 2024; 335: 118604.
36. Yao D, Bao L, Wang S, Tan M, Xu Y, Wu T, *et al.* Isoliquiritigenin alleviates myocardial ischemia-reperfusion injury by regulating the Nrf2/HO-1/SLC7a11/GPX4 axis in mice. Free Radic Biol Med 2024; 221: 1–12.
37. Feng Q, Yang Y, Qiao Y, Zheng Y, Yu X, Liu F, *et al.* Quercetin ameliorates diabetic kidney injury by inhibiting ferroptosis via activating Nrf2/HO-1 signaling pathway. Am J Chin Med 2023; 51:997–1018.
38. Peng C, Ai Q, Zhao F, Li H, Sun Y, Tang K, *et al.* Quercetin attenuates cerebral ischemic injury by inhibiting ferroptosis via Nrf2/HO-1 signaling pathway. Eur J Pharmacol 2024; 963: 176264.
39. He W, Su Q, Liang J, Sun Y, Wang X, Li L. The protective effect of nicorandil on cardiomyocyte apoptosis after coronary microembolization by activating Nrf2/HO-1 signaling pathway in rats. Biochem Biophys Res Commun 2018; 496: 1296–1301.
40. Liang J, Li L, Sun Y, He W, Wang X, Su Q. The protective effect of activating Nrf2/HO-1 signaling pathway on cardiomyocyte apoptosis after coronary microembolization in rats. BMC Cardiovasc Disord 2017; 17: 272.
41. Qin Z, Kong B, Zheng J, Wang X, Li L. Alprostadil injection attenuates coronary microembolization-induced myocardial injury through GSK-3β/Nrf2/HO-1 signaling-mediated apoptosis inhibition. Drug Des Devel Ther 2020; 14: 4407–4422.